Heliyon 10 (2024) e30887

Contents lists available at ScienceDirect

Heliyon

journal homepage: www.cell.com/heliyon

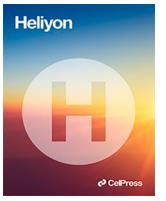

Case report

Skeletal overgrowth in a pre-pubescent child treated with pan-FGFR inhibitor

Fataneh Majlessipour [a,1], Gaohui Zhu [b,c,1], Nicole Baca [a], Meenasri Kumbaji [c], Vivian Hwa [c,d,e,*], Moise Danielpour [f,**]

[a] *Pediatric Hematology and Oncology, Cedars-Sinai Guerin Children's and Cedars-Sinai Cancer, Los Angeles, CA, 90048, USA*
[b] *Department of Endocrinology Children's Hospital of Chongqing Medical University, National Clinical Research Center for Child Health and Disorders, Ministry of Education Key Laboratory of Child Development and Disorders, Chongqing, 400014, China*
[c] *Division of Endocrinology, Cincinnati Children's Hospital Medical Center, Department of Pediatrics, University of Cincinnati College of Medicine, Cincinnati, OH, 45229, USA*
[d] *Department of Pediatrics, University of Cincinnati College of Medicine, Cincinnati, OH, 45229, USA*
[e] *Premium Research Institute for Human Metaverse Medicine (WPI-PRIMe), Osaka University, Osaka, Japan*
[f] *Maxine Dunitz Neurosurgical Institute at the Department of Neurosurgery, Cedars-Sinai Guerin Children's, Los Angeles, CA, 90048, USA*

ARTICLE INFO

Keywords:
Skeletal overgrowth
Fibroblast growth factor receptor
Fibroblast growth factor receptor inhibitor
Neuroglial tumor
Insulin-like growth factor
Skeletal dysplasia
Skeletal deformity

ABSTRACT

Fibroblast growth factors and their receptors (FGFR) have major roles in both human growth and oncogenesis. In adults, therapeutic FGFR inhibitors have been successful against tumors that carry somatic FGFR mutations. In pediatric patients, trials testing these anti-tumor FGFR inhibitor therapeutics are underway, with several recent reports suggesting modest positive responses. Herein, we report an unforeseen outcome in a pre-pubescent child with an FGFR1-mutated glioma who was successfully treated with FDA-approved erdafitinib, a pan-FGFR inhibitor approved for treatment of Bladder tumors. While on treatment with erdafitinib, the patient experienced rapid skeletal and long bone overgrowth resulting in kyphoscoliosis, reminiscent of patients with congenital loss-of-function *FGFR3* mutations. We utilized normal dermal fibroblast cells established from the patient as a surrogate model to demonstrate that insulin-like growth factor 1 (IGF-1), a factor important for developmental growth of bones and tissues, can activate the PI3K/AKT pathway in erdafitinib-treated cells but not the MAPK/ERK pathway. The IGF-I-activated PI3K/AKT signaling rescued normal fibroblasts from the cytotoxic effects of erdafitinib by promoting cell survival. We, therefore, postulate that IGF-I-activated P13K/AKT signaling likely continues to promote bone elongation in the growing child, but not in adults, treated with therapeutic pan-FGFR inhibitors. Importantly, since activated MAPK signaling counters bone elongation, we further postulate that prolonged blockage of the MAPK pathway with pan-FGFR inhibitors, together with actions of growth-promoting factors including IGF-1, could explain the abnormal skeletal and axial growth suffered by our pre-pubertal patient during systemic therapeutic use of pan-FGFR inhibitors. Further studies to find more targeted, and/or appropriate dosing, of pan-FGFR inhibitor therapeutics for children are essential to avoid unexpected off-target effects as was observed in our young patient.

* Corresponding author. Premium Research Institute for Human Metaverse Medicine (WPI-PRIMe) Osaka University, Osaka, Japan.
** Corresponding author. Maxine Dunitz Neurosurgical Institute Department of Neurological Surgery Guerin Children's at Cedars-Sinai Medical Center Los Angeles, California, 90048, USA.
E-mail addresses: hwa.vivian.prime@osaka-u.ac.jp (V. Hwa), Moise.Danielpour@cshs.org (M. Danielpour).
[1] Both lead authors contributed equally to this work.

https://doi.org/10.1016/j.heliyon.2024.e30887
Received 3 September 2023; Received in revised form 3 May 2024; Accepted 7 May 2024
Available online 19 May 2024

1. Introduction

Fibroblast growth factors (FGF) 1–23 and their receptors (FGFR) 1–4 participate in complex signaling cascades that regulate human growth, development, and metabolism. FGFR 1–4 are structurally similar to other members of the extensive tyrosine kinase receptor family, consisting of an extracellular ligand-binding domain, a single transmembrane domain, and an intracellular tyrosine kinase region involved in signal transduction. The binding of FGF to FGFR triggers the activation of multiple signaling pathways including the mitogen-activated protein kinase (MAPK) pathway, phosphoinositide 3-kinase (PI3K), and signal transducer and activator of transcription (STAT) pathways [1]. Pathological genetic variants in each of the four FGFR have been described and are known to have profound biological effects, either globally (congenital variants) or targeted (somatic variants). For example, FGFR3 is established as an important negative regulator of bone growth since congenital activating (gain-of-function) *FGFR3* variants are causal of achondroplasia, a severe form of skeletal dwarfism in which ligand-independent, constitutive, MAPK activation significantly impairs bone elongation [2,3], while congenital loss-of-function *FGFR3* variants can cause abnormal bone elongation associated with CATSHL Syndrome (camptodactyly, tall stature, scoliosis, and hearing loss) [4].

In cancers, somatic activating *FGFR* variants are well-known drivers of malignant transformation and cell growth. Rosette-forming glioneuronal tumor (RGNT), a rare type of central nervous system (CNS) neoplasia, has been attributed to constitutive activation of FGFR signaling due to mutations within the kinase domain of FGFR1 [5]. In adult patients, FGFR inhibitors are effective against some tumors carrying activating *FGFR* gene mutations and fusions. In contrast, the efficacy of therapeutic FGFR inhibitors in pediatric patients with recurrent gliomas harboring *FGFR* mutations is limited, albeit emerging [6–8]. Erdafitinib (JNJ-427564493) is one such inhibitor and is the first pan-FGFR inhibitor approved by the Food and Drug Administration (FDA) for adult patients with urothelial/bladder cancer [9]. In adults, the most common toxicities associated with erdafitinib and other FGFR inhibitors include hyperphosphatemia, skin, and nail toxicities, as well as hand and foot syndrome (redness, swelling, peeling, or tenderness on the hands or feet) [10].

With the increased use of targeted antineoplastic therapies in pediatric patients [7,8,11–15], the downstream and on-target off--tumor effects may pose new challenges. The potential global inhibition of FGFR signaling cascades in pre-pubertal and pubertal children is of significant concern given the critical role of downstream pathways in normal growth and development. Interestingly, rapid growth had been noted in a few cases although implications and mechanisms of action were not investigated [7,15]. Here, we present the first detailed report of a serious adverse effect involving skeletal and long bone overgrowth during successful erdafitinib treatment of RGNT (due to a somatic *FGFR1*-variant) in a pre-pubertal adolescent male. The pattern of overgrowth and skeletal deformity in our patient is strikingly reminiscent of patients with congenital loss-of-function *FGFR3* mutations [4].

FGFR3 loss-of-function mutations in humans, and mouse models, are known to result in vertebral abnormalities, bone deformities [16], and skeletal overgrowth [17], indicating that the normal function of FGFR-3 is to limit, rather than promote, osteogenesis. Hence pan-FGFR inhibitors mimic *FGFR3* null conditions, wherein the normal limiting osteogenic actions of FGFR would be lost. This, together with growth factors that continue to promote osteogeneses, could explain the unusual bone growth. To investigate how well-known osteogenic growth-promoting factors such as insulin-like growth factor 1 (IGF-I) might continue to function in the presence of pan-FGFR inhibitors, we utilized dermal fibroblasts from our patient as a surrogate *in vitro* cellular model, since osteogenic cells such as chondrocytes were not available from the patient. We discovered that IGF-I can activate erdafitinib-inhibited PI3K/AKT signaling pathway but not erdafitinib-inhibited MAPK/ERK pathway, thus protecting the fibroblasts against programmed cell death. We posit a mechanism whereby IGF-I, a growth factor well documented to be important in growth and development, may also contribute towards skeletal overgrowth and spinal deformity in the presence of the pan-FGFR inhibitor, erdafitinib. We recommend caution and further studies of appropriate FGFR inhibitor application and potential concomitant control of bone growth prior to widespread use in children.

2. Materials and Methods

2.1. Antibodies

Antibodies used were anti-phospho-AKT(Ser 473), anti-phospho-AKT(Thr308), and anti-Phospho-p44/42 MAPK (Erk1/2) (Thr202/Tyr204) rabbit mAb (Cell Signaling Technology, Danvers, MA), anti-Akt (pan) Rabbit mAb, p44/42 MAPK (Erk1/2) (137F5) Rabbit mAb(Cell Signaling Technology, Danvers, MA), anti-PARP rabbit mAb and Cleaved Caspase-3 (Asp175) (5A1E) Rabbit mAb (Cell Signaling Technology, Danvers, MA), anti-alpha tubulin monoclonal horseradish peroxidase conjugate (Cell Signaling Technology, Danvers, MA), Secondary antibodies (horseradish peroxidase-linked anti-rabbit IgG and anti-mouse IgG antibodies) were obtained from Amersham Biosciences (Uppsala, Sweden).

2.2. Cell culture

Primary fibroblasts were established from skin biopsies taken from the patient, in compliance with Institutional Review Boards at Cedars-Sinai Medical Center and Cincinnati Children's Hospital Medical Center. Sanger DNA sequencing confirmed that patient fibroblasts did not carry the somatic *PTPN11* or *FGFR1* variants identified in the tumor. Cells were maintained in Minimum Essential Medium Eagle-alpha modification (α-MEM) supplemented with 15 % fetal bovine serum and 200mM L-glutamine at 37 °C in 5 % CO_2. For experiments, cells were seeded in 6 well-plates and when cell growth reached 70%–80 % confluency, cells were serum starved in

α-MEM supplemented with 0.1 % bovine serum albumin (BSA) for 18 h. Serum-starved cells were pre-treated with Erdafitinib (MedChemExpress, Cat No.HY-18708) at concentrations indicated for 30 min, prior to the addition of FGF2 (R&D Systems, Cat No. 233-FB-01 M), IGF-I (Gibco, Cat No. PHG0078), or IGF2 (R&D Systems, Cat No. 292-G2-050), in co-treatment experiments. The 5 mM erdafitinib concentrated stock solution was dissolved in 2 % DMSO as recommended by the manufacturer. Erdafitinib-free (0 nM) media included 0.005 % DMSO while NC ("negative control") media did not include DMSO, thus controlling for any potential effects of DMSO.

2.3. Osteogenic differentiation of primary human mesenchymal stem cells (hMSC)

Normal adult bone marrow-derived mesenchymal stem cells (#PT-2501) were purchased from Lonza Walkersville Inc., MD, USA. Human Mesenchymal stem cells (hMSCs) were cultured and maintained as recommended in MSCGM™ Mesenchymal stem cell growth medium bulletkit™ (#PT-3001, Lonza Walkersville Inc., MD, USA). Differentiation of osteogenic lineages from hMSCs was initiated using Human Mesenchymal Stem Cell (hMSC) Osteogenic differentiation Medium BulletKit™ (#PT-3002, Lonza Walkersville Inc., MD, USA) on collagen I coated 6 well cell culture plates. Differentiation protocol was adopted from the instructions provided for hMSCs by Lonza. Cells were utilized after 4–5 weeks of differentiation. All the cell lines were maintained in a 37 °C, 5 % CO_2 humidified incubator.

For erdafitinib treatments, hMSCs and osteogenic differentiated cells were starved in DMEM/F12 (#11330057, Life Technologies, CA, USA) with 0.1 % BSA and 1 % Penicillin- Streptomycin (#15140-122, Life Technologies, CA, USA) for 18hrs. After starvation, cells were pre-treated with 0.005 % DMSO and Erdafitinib 200nM for 30mins. Recombinant Human IGF1 100ng/mL (#291-G1, R&D systems, MN, USA) was added to Erdafitinib 200nM treated wells for 2 hours. Cells were then washed with cold PBS and cell lysates were collected for immunoblot analysis.

2.4. Alizarin Red S stain for calcium deposits to detect osteogenic induction

Differentiated osteogenic lineage and hMSCs were washed with Dulbecco's PBS without Ca^{2+}/Mg^{2+}(#14190144, Life Technologies, CA, USA) followed by 30mins fixation in 10 % neutral buffered formalin. Cells were washed with distilled water and incubated in 2 % Alizarin Red S stain (#A5533-25G, Sigma-Aldrich, MO, USA) solution at PH 4.1–4.3 for 45 minutes at room temperature in the dark. Cells were washed with distilled water four times. After the addition of DPBS, cells were microscopically analyzed for calcium deposits using Olympus CKX53 (OLYMPUS, Tokyo, Japan).

2.5. Western immunoblotting

Cells were solubilized in Sigma M2 Cell Lysis Buffer (pH 7.5, 50 mM tris(hydroxymethyl)aminomethane (Tris), 150nM sodium chloride, 1 mM ethylenediaminetetraacetic acid (EDTA), 1 % Triton-X100) supplemented with a protease inhibitor tablet (Roche Applied Science) and 100 mM sodium orthovanadate. Protein concentrates of the lysates were determined using the Bradford assay, and 20 μg protein was loaded onto a 10 % sodium dodecyl sulfate-polyacrylamide gel electrophoresis gel (SDS-PAGE). The gel-fractionated proteins were then transferred onto nitrocellulose membranes and blocked using 5 % BSA in 1X Tris-buffered saline. Western blots were processed with the appropriate primary and secondary antibodies following the manufacturer's protocols and scanned using the Odyssey IR Imaging System (LICOR Biosciences).

2.6. WST-1 (water-soluble tetrazolium salt) assay

For cell proliferation and survival, fibroblasts were seeded to a 96-wells-plate (flat bottom) at a concentration of 5×10^4 cells/well in a final volume of 100 μl/well of α-MEM supplemented with 15 % fetal bovine serum and 200mM L-glutamine and incubated for 24 hours at 37 °C in 5 % CO2. Cells were serum starved in α-MEM supplemented with 0.1 % BSA for 18 h and then treated with Erdafitinib, FGF2, IGF1, and IGF2. At the time points indicated, 10μl Cell Proliferation Reagent WST-1 (Cat No. 1644807) was added following the manufacturer's instructions. Briefly, cell mixtures were incubated for 1 hour at 37 °C and 5 % CO2, and shaken for 1 min on a shaker, prior to absorbance measurements at 450 nm absorbance wavelength and 690 nm reference wavelength.

3. Results

3.1. Clinical history

A 19-year-old male was initially diagnosed at age 9 with a pilomyxoid astrocytoma with leptomeningeal dissemination and underwent chemotherapy with partial response both at the initial diagnosis and time of first progression. At the second progression (at the age of 14 years and ten months) he underwent an open biopsy. Next-generation gene sequencing of the tumor was performed at Cedars-Sinai Medical Center (CSMC), Los Angeles, and the University of California San Francisco (UCSF). Both institutions identified an activating FGFR 1 variant, which is consistent with a molecular diagnosis of RGNT. An activating Protein Tyrosine Phosphatase Non-Receptor Type 11 (*PTPN11 c.181G > C*, p.Asp61His) mutation was also identified. He was enrolled in the Pediatric MATCH (Molecular Analysis for Therapy Choice) Screening Study APEC1621SC (NCT03155620) and central review confirmed FGFR1 gene variant (heterozygous *FGFR1 c.1966A > G*, p.Lys656Glu) suitable for treatment with erdafitinib (JNJ-42756493). He enrolled on

APEC1621B (NCT03210714) and started treatment with Erdafitinib at the age of 15 years and four months [18]. At the time, his Tanner staging was delayed and estimated at stage 2–3. The initial daily dose of 7 mg erdafitinib, taken orally for 5 months, required frequent interruptions of therapy due to high phosphorus levels (Table 1) and requiring administration of high doses of oral phosphate binders. He was not on any glucocorticoids during the erdafitinib treatment. When he transferred care, due to relocation, the dose of erdafitinib was reduced to 5 mg daily resulting in fewer treatment interruptions.

Despite a remarkable tumor response, with an approximately 80 percent reduction in tumor volume and contrast enhancement on magnetic resonance imaging or MRI (Supplemental Fig. 1) erdafitinib had to be discontinued due to the patient's unusual rapid growth over the 9 months of therapy, severe kyphoscoliosis, and spinal cord compression with cervical myelopathy. The patient grew a total of 14.3 cm, or at an annualized growth of 19.06 cm (normal growth is ~10 cm per year for a 15-year-old male). Growth prior to erdafitinib therapy was at the 16th to 25th percentile for height and shifted to the 70th percentile during therapy (Fig. 1). The rapid growth led to skeletal deformities which were visible on X-rays, when compared to normal cervical and thoracic spine before erdafitinib treatment (Fig. 2A–a to c). Cervical lordosis and thoracic scoliosis were evident after 9 months of erdafitinib treatment (Fig. 2A, d-i). MRI imaging of the cervical, thoracic and lumbar spine showed the development of deformities after commencing systemic erdafitinib therapy (Fig. 2B–a-d). Of note, he also developed hip flexor contractures not visualized on the imaging, resulting in an underestimation of his height measurements. The cranial vault (membranous bone), unlike cartilaginous skeletal bones, appeared to be unaffected. He returned to our medical center for surgical correction of his symptomatic kyphoscoliosis after cessation of therapy

Table 1
Clinical biochemistry profile at the age of 16.2 years, one month after cessation of erdafitinib.

Tests	Patient's Values	Normal Values
Testosterone Free	1.1 pg/mL	18-111.0 pg/mL
Testosterone Total	13 ng/dL	Male prepubertal stage I: <5 ng/dL Male pubertal stage II: <67 ng/dL Male pubertal stage III: 21-719 ng/dL Male pubertal stage IV: 25-912 ng/dL Male pubertal stage V: 110-975 ng/dL
Growth Hormone	2.7 ng/mL	<10.1 ng/mL
IGF-2	621 ng/dL	Prepubertal: 258-882 ng/mL Pubertal: 273-872 ng/mL
IGF-1	256 ng/mL	Age (years) / Male Pubertal Stages: I; II & III; IV & V IGF-1 in ng/mL 10-10.9: 84-315; 78-418; 349-817 11-11.9: 96-341; 101-478; 318-765 12-12.9: 109-368; 127-543; 289-716 13-13.9: 123-396; 158-614; 262-668 14-14.9: 138-426; 192-689; 236-622 15-15.9: 153-457; 230-769; 212-578
Z- Score	-1.7	-2 to +2
IGF binding protein-3 (IGFBP-3)	5.8 mg/dL	3.4-9.5 mg/dL
Glucose	84 mg/dL	70-99 mg/dL
Electrolytes		
Magnesium	1.9 mg/dL	1.7-2.2 mg/dL
Phosphorus	3.7 mg/dL	2.3-4.7 mg/dL
Calcium	9.6 mg/dL	8.4-10.2 mg/dL
Potassium	3.8 mmol/L	3.5-5.0 mmol/L
Sodium	135 mmol/L	135-145 mmol/L
Kidney Function		
BUN	17 mg/dL	8.4-21 mg/dL
Creatinine	0.4 mg/dL	0.65-1.04 mg/dL
Liver Function		
Total bilirubin	0.3 mg/dL	0.3-1.2 mg/dL
Alkaline phosphatase	746 U/L	89-365 U/L
ALT	22 U/L	0-55 U/L
AST	27 U/L	5-34 U/L

Series 11, No. 246 □ Page 29

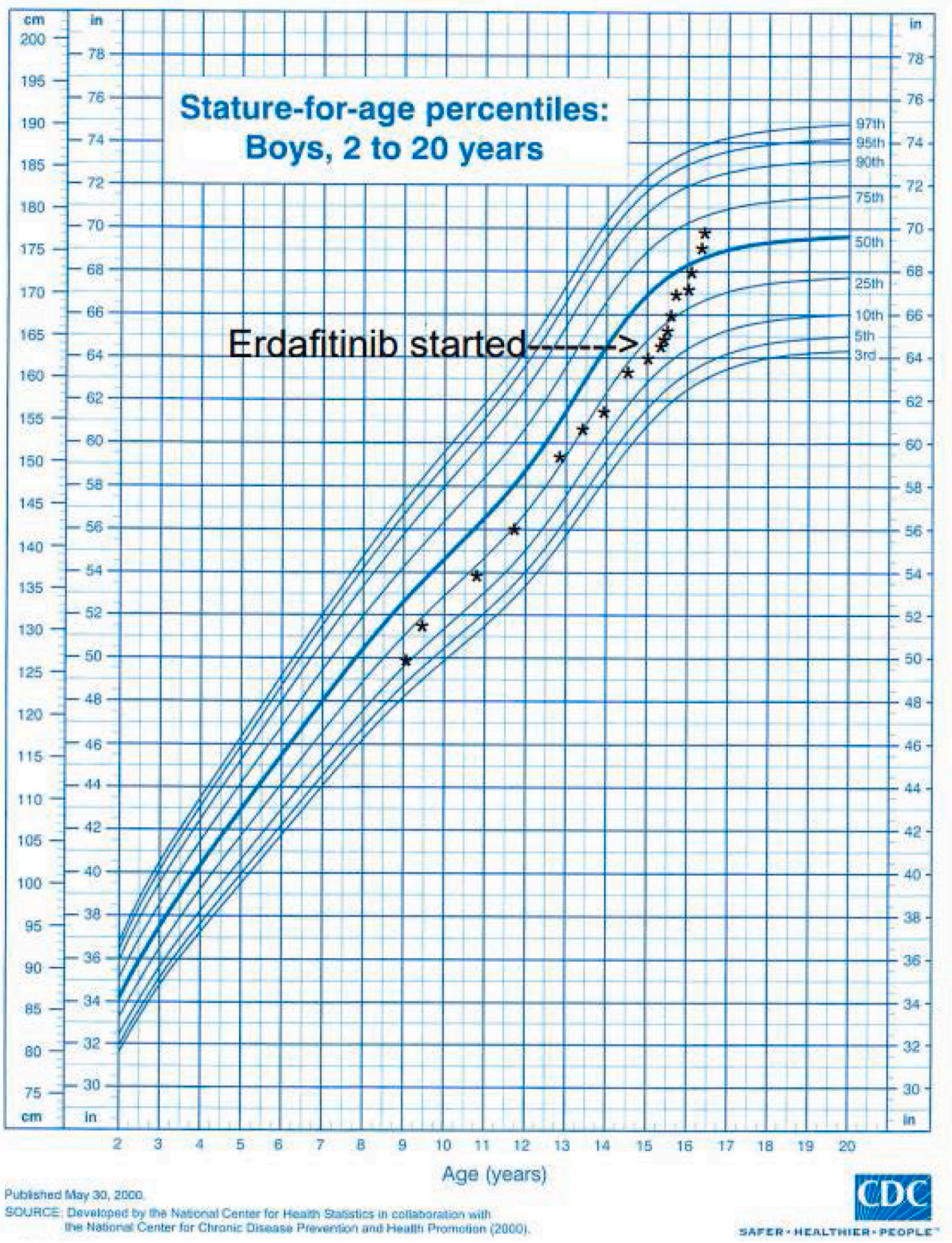

Fig. 1. Male growth chart demonstrating the patient's growth prior to starting erdafitinib as well as the rapid growth after starting erdafitinib.

(Fig. 2B–e).

Following the cessation of erdafitinib, bone density by dual-energy x-ray absorptiometry (DEXA) bone scan, was performed. The mean bone density value for the lumbar spine measured 0.6322 gm/sq.cm, which is −3.8 standard deviation below the mean value for the age-matched population and more than 2.5 standard deviations below the value for males at peak bone mass. These findings were consistent with osteoporosis. However, since a baseline DEXA scan was not performed prior to erdafitinib therapy, it remains unclear if the osteoporosis was independent of erdafitinib therapy or if therapy was a contributor.

Bone age assessments had not been performed prior to or during erdafitinib therapy. At cessation of therapy, bone age [19] was determined to be 14 years at the chronological age of 16.2 years, which is greater than 2 standard deviations below the mean. At the age of 17 years and 5 months, more than 15 months after cessation of therapy, bone age remained 2 years delayed.

His serum markers for growth (i.e., growth hormone or GH, IGF-I, and IGF binding protein-3, IGFBP-3), at age 16 years 3 months were within normal ranges for a male with pubertal stage II-III. Total testosterone level was consistent with the early pubertal stage, although free testosterone was low. A metabolic panel showed serum alkaline phosphatase of 746 U/L was significantly elevated above the normal range (89–365 U/L; Table 1). The high alkaline phosphatase level was likely reflective of increased bone metabolism and not liver damage as markers of liver functions were normal (Table 1).

3.2. *Patient-derived fibroblasts, an in vitro surrogate model for investigating erdafitinib-inhibited FGFR signaling*

The unusual rapid skeletal growth in our patient (Figs. 1 and 2) whilst on systemic pan-FGFR inhibitor erdafitinib, strongly indicated that erdafitinib had off-target effects, most prevalently involving cartilaginous bone. Since it is well established that normal FGFR signaling limits osteogenic growth, we posit that, at least in our patient, it is the combination of erdafitinib-mediated blockage of FGFR signaling and the continued availability of osteogenic growth-promoting factors such as IGF-I, which may have led to the unchecked skeletal overgrowth seen in the patient (Supplemental Fig. 1). Osteogenic cells such as osteoblasts or chondrocytes were not available from our patient to test this hypothesis. However, since erdafitinib specifically interacts with FGFRs and prevents ligand-induced signaling in all FGFR-carrying cell types, we utilized fibroblasts established from our patient as a surrogate model to assess the effects of IGF-I in the presence of erdafitinib. We took advantage of the ease of fibroblast cell cultivation and its ready responsiveness to many factors including IGFs and FGF2 (aka basic FGF, bFGF), a ligand that activates all four FGFRs [20,21].

We first confirmed that the fibroblasts, as well as whole blood and spinal disc material removed from the patient during surgery, did not carry the somatic activating *FGFR1* or *PTPN11* variants identified in his RGNT (Supplemental Fig. 3). We next assessed erdafitinib inhibition of FGFR signaling in the patient's fibroblasts, focusing on the PI3K/AKT and MAPK/ERK pathways. By immunoblot

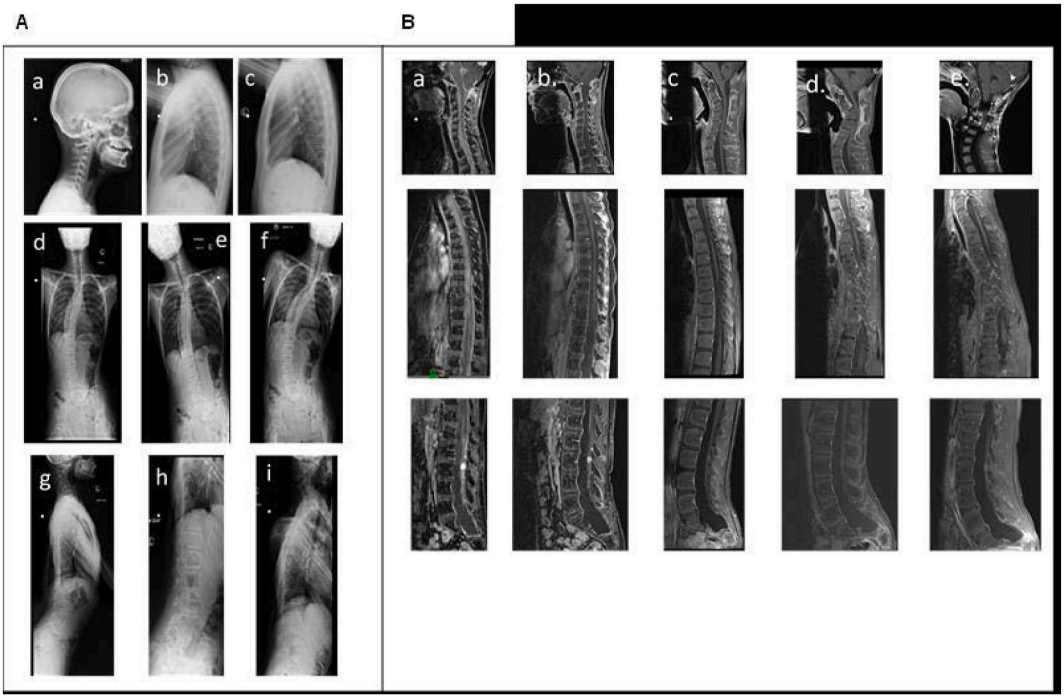

Fig. 2. Abnormal rapid skeletal growth in a patient treated with erdafitinib, a pan-FGFR inhibitor. **A.** X-ray of the cervical and thoracic spine before treatment (***a, b, and c***) and 9 months after treatment (***d, e, f, g, h, and i***) with erdafitinib showing the development of cervical lordosis and thoracic scoliosis. **B.** MRI images (sagittal, T1 post- Contrast Fat saturation (FS) pulse sequences) of the cervical, thoracic, and lumbar spine demonstrating the development and progression of spinal deformities after commencing erdafitinib: ***a.*** Baseline; ***b.*** at 2 months; ***c.*** at 5 months; ***d.*** at 9 months; ***e.*** at 12 months which was 3 months after cessation of erdafitinib and after cervical deformity surgical correction.

analyses, we discovered that in untreated fibroblasts, ERK1/2 (Extracellular Signal Receptor Regulated Kinase 1 and 2), a member of the MAPK family, was already robustly activated (pERK1/2; Fig. 3A–a, NC, normal control that lacked the DMSO used for solubilization of erdafitinib, and 0 nM erdafitinib control which contain DMSO, see Materials and Method). Basal activated AKT (both pAKT-T308 and pAKT-S473) was also detectable (Fig. 3A–a, NC and 0 nM erdafitinib controls). Erdafitinib treatment at 100 nM, a concentration that inhibited FGFR signaling in many cancer cell lines [22], was sufficient to reduce activated pERK1/2 dramatically and pAKT with no further reductions were detected when fibroblasts were treated with 200 nM or 300 nM erdafitinib (Fig. 3A–a). Since erdafitinib is a specific pan-inhibitor of activated FGFRs, our results implied that FGFR-mediated signaling appears to be constitutively activated in our human dermal fibroblasts, at least under our experimental conditions. Of note, we routinely detected robust basal pERK1/2 in unrelated primary human dermal fibroblast cell lines [23], suggesting constitutive activated FGFR signaling is a normal phenomenon for primary human fibroblasts, potentially as an autocrine/paracrine response to cellular FGF production.

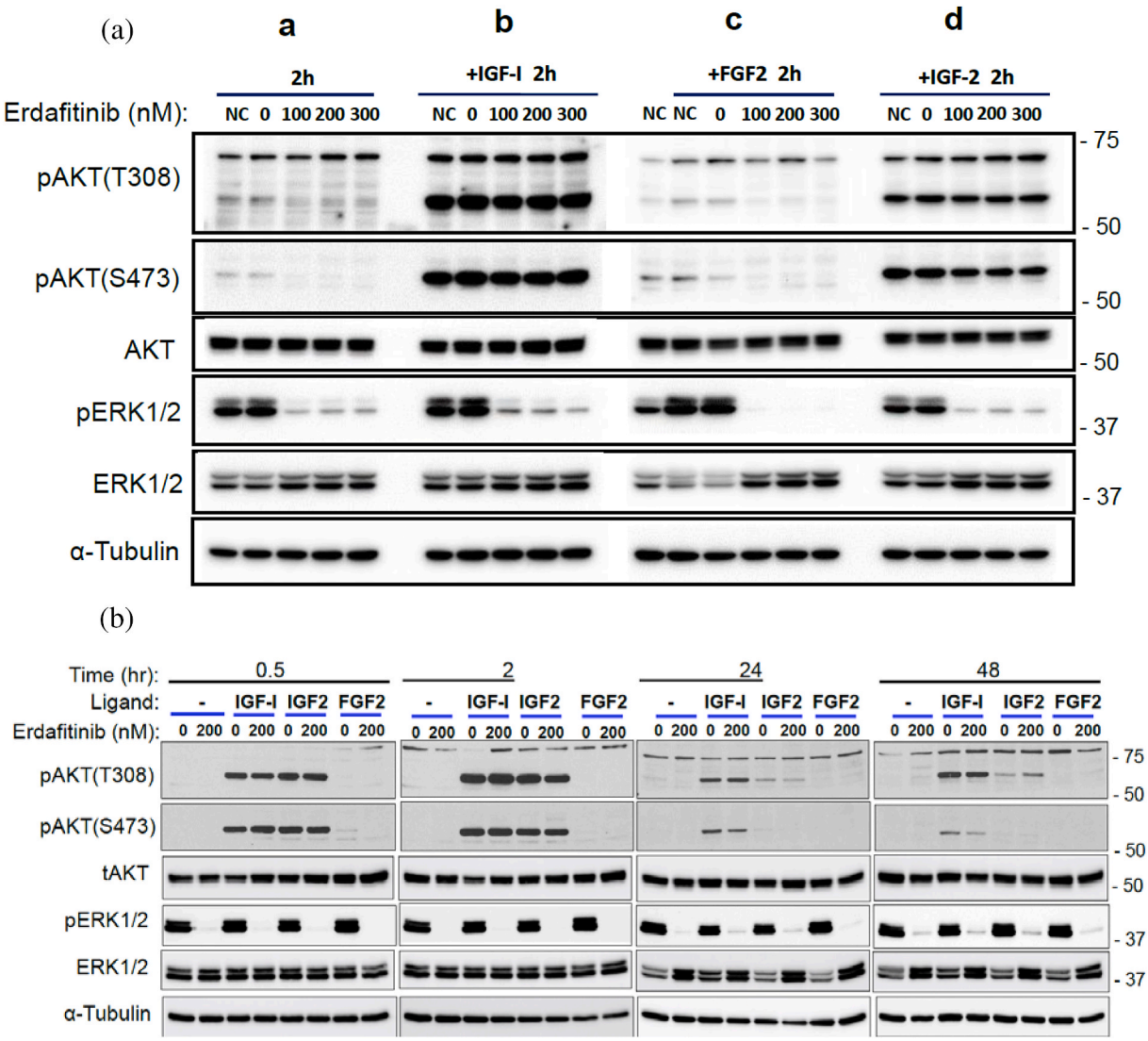

Fig. 3. A: Immunoblot analysis of MAPK and PI3K/AKT signaling in the presence of increasing doses of erdafitinib, growth factors- In untreated fibroblasts, ERK1/2 and AKT (both pAKT-T308 and pAKT-S473) are activated (in NC, normal control (no DMSO), 0 nM erdafitinib but with DMSO), Erdafitinib treatment at 100 nM dramatically reduce activated pERK1/2 and pAKT with no further reductions detected when fibroblasts were treated with 200 nM or 300 nM erdafitinib **(3A-a)**. Erdafitinib-inhibited pERK1/2 was not re-activated by the co-addition of IGF-I (**3A-b**), FGF2 (**3A-c**) or IGF-2 (**3A-d**). AKT signaling pathway (pAKT-T308 and pAKT-S473) were consistently activated by IGF-I and IGF-2, but not by FGF2 (**3A**), at all concentrations of erdafitinib tested (100 nM–300 nM) (see Supplementary Material Fig. 3A-uncropped.)
Fig. 3.B: immunoblot analysis of signaling response in the presence of erdafitinib and growth factors over time- Fibroblasts were co-treated with 200nM erdafitinib and growth factors (IGF-1, IGF-2, FGF-2) for 0.5, 2, 24, 48 hours. Only with IGF-I treatment, activation of AKT was sustained for 48 hours. our data suggest, in our patient fibroblasts, that IGF-I activation of AKT signaling is sustained and independent of the FGFR signaling inhibitory effects of erdafitinib. (see Supplementary Material Fig. 3B-uncropped.).

3.3. IGF-I activates AKT but not ERK1/2 in erdafitinib-treated fibroblasts

Erdafitinib suppressed the robust basal pERK1/2 in our patient's primary fibroblasts (Fig. 3A), an FGFR signaling inhibitory effect predicted for all cell types responsive to FGFs including cartilaginous cells. To assess if growth factors can counter the erdafitinib-inhibited signaling effects, we evaluated the impacts of IGF-I, the closely related IGF-2, and FGF2, on erdafitinib-treated fibroblasts. Erdafitinib-inhibited pERK1/2, intriguingly, was not re-activated by the co-addition of IGF-I (Fig. 3A–b), FGF2 (Fig. 3A–c) or IGF-2 (Fig. 3A–d). However, the AKT signaling pathway (pAKT-T308 and pAKT-S473) was robustly and consistently activated by IGF-I and IGF-2, but not by FGF2 (Fig. 3A), at all concentrations of erdafitinib tested (100 nM–300 nM).

The activation of AKT by IGFs in erdafitinib-treated fibroblasts was readily detected 2 hours post-treatment. To determine time-dependent signaling responses, fibroblasts were co-treated with 200nM erdafitinib and growth factors for up to 48 hours (Fig. 3B). Within 30 min of exposure to IGF-I or IGF-2, robust pAKT was detected. Only with IGF-I treatment, however, was activation of AKT sustained for 48 hours (Fig. 3B). Altogether, our data suggest that in our patient fibroblasts, IGF-I activation of AKT signaling is sustained and independent of the FGFR signaling inhibitory effects of erdafitinib.

While we did not have primary cartilaginous cells, we did utilize a human osteogenic-like model (differentiated primary human

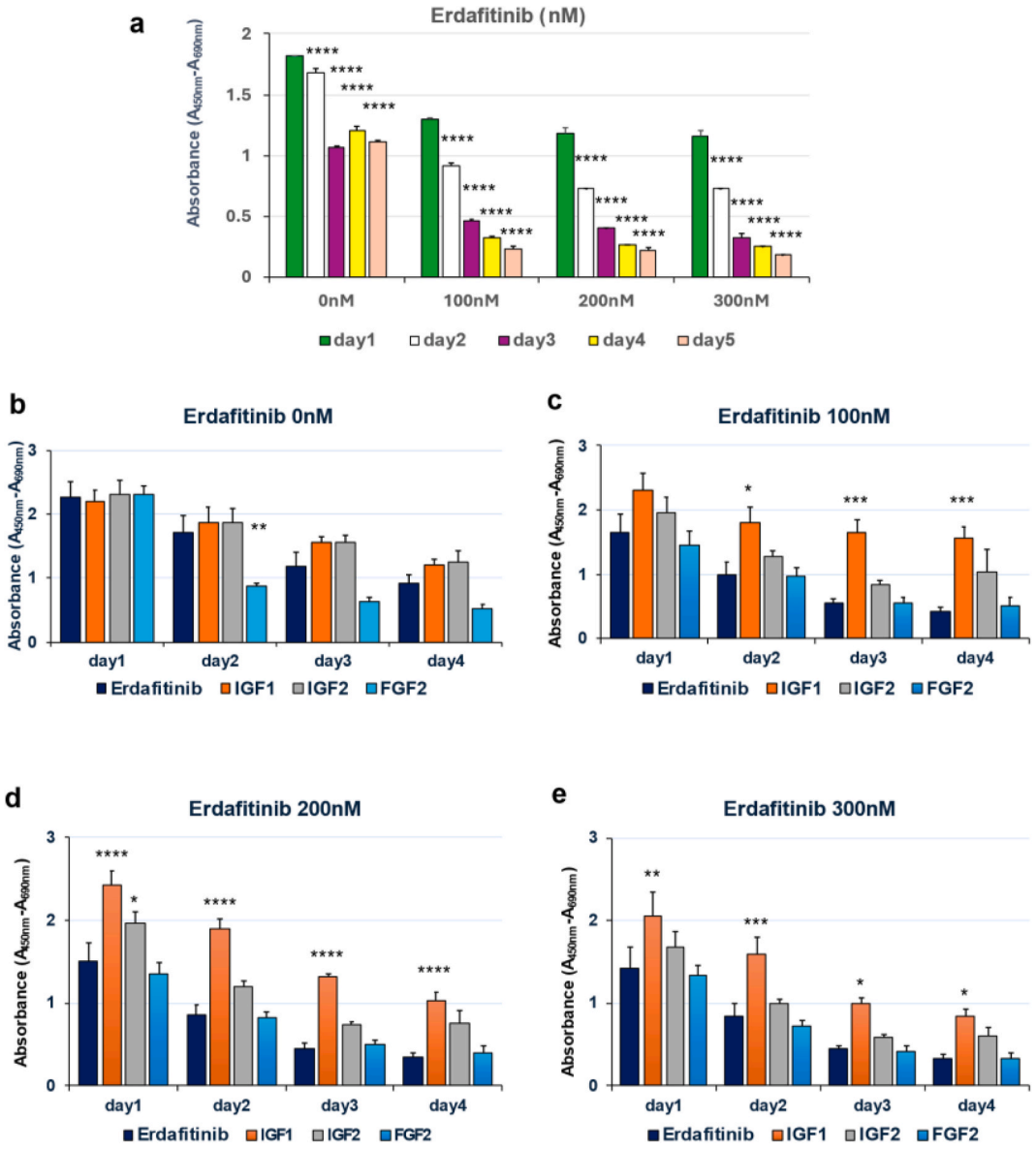

Fig. 4. Survival/viability assay (WST-1) in response to erdafitinib doses over time at a cell density of 5x104 cells/well [**4a**]; WST-I of cells treated with IGF-I, FGF2, or IGF-2 only [**4b**]; WST-1 of cells treated with increasing concentration of erdafitinib and co-treated with IGF-I, IGF-2, or FGF2 **(4c, 4d, 4e)**. SEM was calculated using Dunnett's multiple comparison test. *p < 0.05, **p < 0.005, ***p < 0.001, ****p < 0.0001.

mesenchymal stem cells, hMSC (Supplemental Fig. 4), to compare erdafitinib and IGF-I-induced signaling effects to our patient's fibroblasts. In the differentiated osteogenic-like cells, pAKT and pERK1/2 were already activated in the absence of erdafitinib, and erdafitinib treatment strongly suppressed both pAKT and pERK (Supplemental Fig. 4). Similar to our patient-derived fibroblasts, co-treatment with IGF-I robustly activated pAKT but not pERK (Supplemental Fig. 4). Hence, our patient's fibroblasts appear to be an appropriate surrogate for assessing the off-target signaling effects of erdafitinib on all normal cells, including bone cells.

3.4. *Growth-promoting IGF-I protects the viability of erdafitinib-treated fibroblasts*

We next assessed whether the biological consequences of the erdafitinib-inhibited FGFR signaling, counteracted by IGF-I, in the patient's fibroblasts, could mimic the enhanced osteogenic growth observed *in vivo*. However, we found that for our primary fibroblasts, *in vitro* cell viability assays proved to be more robust and reproducible than proliferation assays. In the viability assay, erdafitinib at all doses (100–300 nM) significantly reduced cell viability to less than 30 % by day 5 of evaluation (Fig. 4a). In the absence of erdafitinib (0 nM), FGF2 (40 ng/ml) treatment, contrary to expectation, also reduced fibroblast viability when compared to untreated, although this reduction was statistically significant only on Day 2 (Fig. 4b). Interestingly, co-treatment with erdafitinib did not alter FGF2-mediated reduction in cell viability (Fig. 4c-e).

In contrast to FGF2, the survival of erdafitinib-free (0 nM) fibroblasts treated with either IGF-I (100ng/ml) or IGF-2 (100ng/ml) was comparable to control (Fig. 4b). However, erdafitinib reduced cell viability was significantly alleviated when fibroblasts were co-treated with IGF-I (Fig. 4c-e). The effects of IGF-2 were less consistent although there was a protective trend. Collectively, our results indicated that, in normal fibroblasts, one biological consequence of erdafitinib inhibition of FGFR signaling is a significant reduction in cell viability which can be counteracted by IGF-I co-treatment.

3.5. *Erdafitinib-induced apoptosis in patient fibroblasts can be reversed by IGF-I*

We determined whether the erdafitinib-induced decrease in fibroblast viability could be due to apoptosis. After treatment with erdafitinib for 24 hours and 48 hours, apoptosis markers, PARP (poly ADP-ribose polymerase), and cleaved caspase 3 were readily detected on immunoblot analysis when compared to controls (Fig. 5). Strikingly, IGF-I treatment strongly suppressed erdafitinib-induced apoptosis (Fig. 5). Notably, IGF-I suppression of erdafitinib-induced apoptosis correlates to sustained IGF-I-inducted AKT signaling (Fig. 3B).

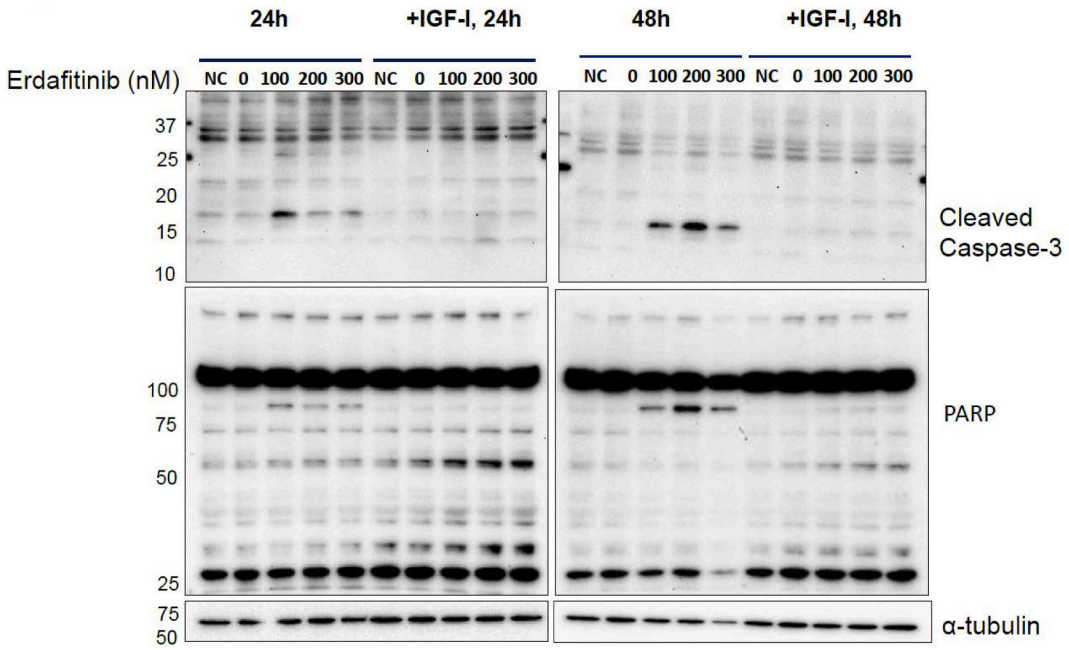

Fig. 5. Immunoblot analysis of apoptosis markers, PARP, and cleaved caspase 3, after 24 hr or 48 hr treatment with erdafitinib with or without IGF-I (100 ng/ml). Fibroblasts were grown in alpha-MEM+15 % FBS till ~80 % confluency, serum-starve for 18 hours in alpha-MEM+0.1 % BSA and pre-treated with erdafitinib (0–300 nM) for 30 min, before the addition of indicated growth factors (IGF-I, 100 ng/ml; FGF2, 40 ng/ml; IGF-2, 100 ng/ml). Cell lysates were collected 2 hours post-treatment. For immunoblot analysis, 20 μg/lane were loaded. (see Supplementary Material Fig. 5-uncropped.).

4. Discussion

Our pre-pubescent patient with RGNT caused by a somatic FGFR variant was successfully treated with erdafitinib, a pan-inhibitor of FGFR. Our patient had unexpected adverse effects of rapid skeletal growth during 9 months of treatment, leading to kyphoscoliosis, and hip flexion contractures. This overgrowth was independent of a pubertal spurt as endocrine values (serum GH, IGF-I, IGFBP-3, testosterone) were more consistent with pre-pubertal status. This phenomenon has been described in other pediatric patients receiving FGFR inhibitors. Stepien and colleagues reported a significant growth hormone-independent growth spurt in a 13-year-old receiving erdafitinib for a recurrent diffuse low-grade glioma [15]. Similarly, Farouk, Sait, and colleagues reported increased linear growth in two pediatric patients, ages 8 and 14 years, who received an oral FGFR 1–3 inhibitor, Debio1347, for low-grade glioma [7].

In vitro studies of molecular pathways important in skeletal growth using our patient-derived normal fibroblast cultures as a surrogate model system, revealed that IGF-1, through activation of the AKT signaling pathway, efficiently rescued the patient's fibroblasts from erdafitinib-induced apoptosis. This suggests that *in vivo* mechanisms involving IGF-I-induced AKT signaling and those of other growth factors such as natriuretic peptide C (CNP), together with inhibition of the normal signaling and functions of FGFR, may contribute to the abnormal over-proliferation and elongation of pre-pubertal bone when erdafitinib is present. We further posit that this skewing towards overgrowth occurs only if the growth plate has not yet fused, as this unusual phenotype has not been reported in adults treated with systemic erdafitinib or other FGFR inhibitors [10].

The systemic erdafitinib treatment in our patient profoundly affected cartilaginous (long bones and growth plate) but not membranous bones (cranial bones). In the growing child, the complex dynamic endochondral ossification process for bone elongation and growth plate maturation is centered around the balance between chondrocyte proliferation and hypertrophy, which also influences bone mineralization, chondrogenic matrix remodeling, and growth plate status [24]. Of the multiple factors and signals, both intrinsic and extrinsic, known to regulate these processes [25], the over 200 pathological variants that disrupt IGF-I production and/or actions, cause proportionate severe short stature [26–28]. These reports support the critical importance of IGF-I-induced signaling for normal bone growth. IGF-I, from circulation and locally produced by the bone [29], acts by binding to the ubiquitous cell surface IGF-1 receptor (IGF1R), a tyrosine kinase receptor in the same superfamily as FGFR [30], and initiates signaling cascades that include the PI3K/AKT and MAPK pathways [31–33] important for cell proliferation and survival [34,35]. In our fibroblast surrogate model, we showed a signaling mechanism whereby sustained IGF-I-induced activation of the PI3K/AKT pathway was sufficient to prevent erdafitinib-mediated cell death, thus providing one signaling mechanism that may contribute to the overgrowth phenotype in our patient and also in CATSHL syndrome [4]. Of noted, *Fgfr3* null mice recapitulated clinical observations of skeletal deformities including kyphosis, and scoliosis as well as curvature and overgrowth of long bones and vertebrae [17]. To overcome the limitation that our patient's fibroblasts are not chondrocytes, future studies will employ human induced pluripotent stem cells (iPSC) generated from our patient fibroblasts, which can subsequently be differentiated to chondrocyte-like cells or cartilaginous bone-like 3D organoid models [36], and together with *in vivo* mouse models, will provide comprehensive *in vitro* and *in vivo* models for further assessment of our hypotheses.

Since only a handful of patients/families diagnosed with CATSHL syndrome due to *FGFR3* loss-of-function mutations have been described to date, consensus for patient management is currently lacking. Our present report suggests potential mechanisms that may explain skeletal abnormalities in growing children when *FGFR* is inactivated (genetically or through pan-FGFR inhibitor treatments), whereby the normal availability of osteogenic growth promoting factors such as IGF-I (or CNP, etc.) act synergistically with loss of FGFR functions. Furthermore, our data suggest that when utilizing therapeutic systemic pan-FGFR inhibitors, judicial use of targeted osteogenic inhibitors, may help avoid adverse effects on the immature skeletal system and should be investigated.

An intriguing insight from our study is whether erdafitinib can be utilized for bone elongation in patients with idiopathic short stature. Germline mutations in FGFR 1–3 cause at least 20 congenital skeletal disorders [37], with achondroplasia, caused by activating (gain-of-function) mutations in *FGFR3* resulting in constitutive activation of the MAPK pathway in chondrocytes which leads to inhibition of endochondral ossification [2,3]. Interestingly, patients with achondroplasia have been treated with recombinant human growth hormone (GH), a key regulator of IGF-I production [26–28] and although GH-induced production of IGF-I is believed to be a key mechanism for increasing growth velocity, final height remains suboptimal [31,38–40]. A potential mechanism for the positive effects of IGF-I was demonstrated in an immortalized mouse chondrocyte cell line model for achondroplasia where IGF-1 prevented constitutively activated FGFR3-mediated apoptosis [31]. However, enhanced GH-induced IGF-I production itself does not appear to be sufficient to override the inhibitory osteogenic effects of activated FGFR-3, and a number of other therapeutics are currently under study [38–40]. Indeed, several FGFR inhibitors have been evaluated *in vitro* and in achondroplasia mouse models with variable results and toxicities [41–43]. Currently, the PROPEL and PROPEL 2 studies, are ongoing to evaluate the safety and efficacy of infigratinib, an FGFR 1–3 inhibitor, as a precision treatment of children with achondroplasia [44].

The FGF/FGFR axis is associated with many types of cancer. Somatic *FGFR1-3* mutations have been identified in pediatric CNS tumors, including gliomas, ependymomas and medulloblastomas [45–47]. Particularly, in pediatric gliomas, *FGFR1* mutations, *FGFR1-TACC1* fusions and *FGFR-TKD* duplications, are well known to result in FGFR1 autophosphorylation resulting in upregulation of the RAS/MAPK pathway [45]. These mutations are expected to be targetable [45]. However, potential serious adverse skeletal growth issues with systemic use of pan-FGFR inhibitors as observed in our patient should be taken into consideration.

The RGNT in our patient also carried an activating *PTPN11* variant in addition to the *FGFR1* mutation. PTPN11 (also known as SHP2) is a signaling molecule that can associate with activated tyrosine kinase receptors such as FGFR and regulate MAPK signaling. An activated PTPN11 is likely to regulate signaling independently of FGFR (and other tyrosine kinase receptors) and, can, therefore, be causal of insensitivity to erdafitinib treatment. However, erdafitinib treatment appeared to have significantly reduced tumor burden in our patient, although RGNT was not completely abrogated as treatment had to be terminated because of adverse growth effects.

5. Conclusion

We report a prepubescent male patient whereby therapeutic erdafitinib, a pan-FGFR inhibitor, significantly reduced the patient's RGNT but treatment was associated with off-target effects of striking skeletal overgrowth that required surgical intervention. In a surrogate cell model utilizing normal fibroblasts established from the patient, erdafitinib, as expected, inhibited FGFR signaling pathways, and led to cellular apoptosis. However, co-treatment with IGF-I, through activation of the AKT signaling pathway, promoted the survival of erdafitinib-treated fibroblasts. Since FGFR signaling inhibits osteogenesis, we postulate that in the bone milieu, prolonged blockage of FGFR signaling with pan-FGFR inhibitors (mimicking loss-of-function *FGFR3* mutations associated with CATSHL syndrome), together with growth-promoting actions of factors including IGF-1, could explain the abnormal skeletal and axial growth suffered by our pre-pubertal patient during systemic therapeutic use of pan-FGFR inhibitors. Further investigations are warranted before the widespread use of systemic FGFR inhibitors for the treatment of FGFR-mutated cancers in prepubescent children.

Work supported by grants

No.

Ethics statement

Written informed consent was obtained in compliance with Institutional Review Boards at Cedars-Sinai Medical Center and Cincinnati Children's Hospital Medical Center including for skin biopsy, subsequent research, and publication of results.

Data availability statement

All data are available in the table, Figures, and supplementary material of the manuscript.

CRediT authorship contribution statement

Fataneh Majlessipour: Writing – review & editing, Writing – original draft, Supervision, Project administration, Investigation, Data curation, Conceptualization. **Gaohui Zhu:** Methodology, Investigation, Formal analysis. **Nicole Baca:** Writing – review & editing, Writing – original draft, Software. **Meenasri Kumbaji:** Methodology. **Vivian Hwa:** Writing – review & editing, Writing – original draft, Validation, Supervision, Resources, Methodology, Investigation, Formal analysis, Data curation, Conceptualization. **Moise Danielpour:** Writing – review & editing, Writing – original draft, Validation, Supervision, Methodology, Formal analysis, Conceptualization.

Declaration of competing interest

The authors declare the following financial interests/personal relationships which may be considered as potential competing interests:Fataneh Majlessipour has patent #USE OF FGFR INHIBITORS FOR TREATMENT OF IDIOPATHIC SHORT STATURE Application number: 17/782,534 pending to Fataneh Majlessipour. Moise Danielpour has patent #USE OF FGFR INHIBITORS FOR TREATMENT OF IDIOPATHIC SHORT STATURE Application number: 17/782,534 pending to Moise Danielpour. Vivian Hwa has patent #USE OF FGFR INHIBITORS FOR TREATMENT OF IDIOPATHIC SHORT STATURE Application number: 17/782,534 pending to Vivian Hwa.

The authors declare that they have no known competing financial interests or personal relationships that could have appeared to influence the work reported in this paper.

Acknowledgments

We would like to thank the patient and his legal guardian who consented to his participation in this study.

Appendix A. Supplementary data

Supplementary data to this article can be found online at https://doi.org/10.1016/j.heliyon.2024.e30887.

References

[1] Y. Xie, N. Su, J. Yang, Q. Tan, S. Huang, M. Jin, et al., FGF/FGFR signaling in health and disease, Signal Transduct. Targeted Ther. 5 (1) (2020) 181.
[2] G.A. Bellus, T.W. Hefferon, R.I. Ortiz de Luna, J.T. Hecht, W.A. Horton, M. Machado, et al., Achondroplasia is defined by recurrent G380R mutations of FGFR3, Am. J. Hum. Genet. 56 (2) (1995) 368–373.

[3] R. Shiang, L.M. Thompson, Y.Z. Zhu, D.M. Church, T.J. Fielder, M. Bocian, et al., Mutations in the transmembrane domain of FGFR3 cause the most common genetic form of dwarfism, achondroplasia, Cell. 78 (2) (1994) 335–342.
[4] R.M. Toydemir, A.E. Brassington, P. Bayrak-Toydemir, P.A. Krakowiak, L.B. Jorde, F.G. Whitby, et al., A novel mutation in FGFR3 causes camptodactyly, tall stature, and hearing loss (CATSHL) syndrome, Am. J. Hum. Genet. 79 (5) (2006) 935–941.
[5] C.G. Lucas, R. Gupta, P. Doo, J.C. Lee, C.R. Cadwell, B. Ramani, et al., Comprehensive analysis of diverse low-grade neuroepithelial tumors with FGFR1 alterations reveals a distinct molecular signature of rosette-forming glioneuronal tumor, Acta Neuropathol Commun 8 (1) (2020) 151.
[6] A.B. Lassman, J.M. Sepúlveda-Sánchez, T.F. Cloughesy, M.J. Gil-Gil, V.K. Puduvalli, J.J. Raizer, et al., Infigratinib in patients with recurrent gliomas and FGFR alterations: a multicenter phase II study, Clin. Cancer Res. 28 (11) (2022) 2270–2277.
[7] Sait S. Farouk, S.W. Gilheeney, T.A. Bale, S. Haque, M.J. Dinkin, S. Vitolano, et al., Debio1347, an oral FGFR inhibitor: results from a single-center study in pediatric patients with recurrent or refractory FGFR-altered gliomas, JCO Precis Oncol 5 (2021).
[8] S. Pant, M. Schuler, G. Iyer, O. Witt, T. Doi, S. Qin, et al., Erdafitinib in patients with advanced solid tumours with FGFR alterations (RAGNAR): an international, single-arm, phase 2 study, Lancet Oncol. 24 (8) (2023) 925–935.
[9] Y. Loriot, A. Necchi, S.H. Park, J. Garcia-Donas, R. Huddart, E. Burgess, et al., Erdafitinib in locally advanced or metastatic urothelial carcinoma, N. Engl. J. Med. 381 (4) (2019) 338–348.
[10] V. Subbiah, S. Verstovsek, Clinical development and management of adverse events associated with FGFR inhibitors, Cell Rep Med 4 (10) (2023) 101204.
[11] I.F. Pollack, S. Agnihotri, A. Broniscer, Childhood brain tumors: current management, biological insights, and future directions, J. Neurosurg. Pediatr. 23 (3) (2019) 261–273.
[12] S.J. Forrest, B. Geoerger, K.A. Janeway, Precision medicine in pediatric oncology, Curr. Opin. Pediatr. 30 (1) (2018) 17–24.
[13] M. Wong, C. Mayoh, L.M.S. Lau, D.A. Khuong-Quang, M. Pinese, A. Kumar, et al., Whole genome, transcriptome and methylome profiling enhances actionable target discovery in high-risk pediatric cancer, Nat. Med. 26 (11) (2020) 1742–1753.
[14] A. Gupta, T.P. Cripe, Immunotherapies for pediatric solid tumors: a targeted update, Paediatr Drugs 24 (1) (2022) 1–12.
[15] N. Stepien, L. Mayr, M.T. Schmook, A. Raimann, C. Dorfer, A. Peyrl, et al., Feasibility and antitumour activity of the FGFR inhibitor erdafitnib in three paediatric CNS tumour patients, Pediatr. Blood Cancer 71 (3) (2024) e30836.
[16] M.P. McDonald, K.M. Miller, C. Li, C. Deng, J.N. Crawley, Motor deficits in fibroblast growth factor receptor-3 null mutant mice, Behav. Pharmacol. 12 (6–7) (2001) 477–486.
[17] J.S. Colvin, B.A. Bohne, G.W. Harding, D.G. McEwen, D.M. Ornitz, Skeletal overgrowth and deafness in mice lacking fibroblast growth factor receptor 3, Nat. Genet. 12 (4) (1996) 390–397.
[18] Lee Alice, P. Mickey Williams, Sinchita Roy-Chowdhuri, David R. Patton, Brent D. Coffey, Joel M. Reid, Jin Piao, Lauren Saguilig, Allen Alonzo Todd, Stacey L. Berg, Alok Jaju, Elizabeth Fox, Douglas S. Hawkins, Margaret M. Mooney, Naoko Takebe, James V. Tricoli, Katherine A. Janeway, Nita Seibel, Donald Williams Parsons, Erdafitinb in patients with FGFR-altered tumors: results from the NCI-COG Pediatric MATCH trial arm B (APEC1621B), J. Clin. Oncol. 41 (16) (2023) 10007–11007.
[19] S.I. Pyle, A.M. Waterhouse, W.W. Greulich, Attributes of the radiographic standard of reference for the national health examination survey, Am. J. Phys. Anthropol. 35 (3) (1971) 331–337.
[20] L.L. Root, G.D. Shipley, Normal human fibroblasts produce membrane-bound and soluble isoforms of FGFR-1, Mol. Cell Biol. Res. Commun. 3 (2) (2000) 87–97.
[21] D.M. Dolivo, S.A. Larson, T. Dominko, FGF2-mediated attenuation of myofibroblast activation is modulated by distinct MAPK signaling pathways in human dermal fibroblasts, J. Dermatol. Sci. 88 (3) (2017) 339–348.
[22] T.P.S. Perera, E. Jovcheva, L. Mevellec, J. Vialard, D. De Lange, T. Verhulst, et al., Discovery and pharmacological characterization of JNJ-42756493 (erdafitinib), a functionally selective small-molecule FGFR family inhibitor, Mol. Cancer Therapeut. 16 (6) (2017) 1010–1020.
[23] A. Rughani, D. Zhang, K. Vairamani, A. Dauber, V. Hwa, S. Krishnan, Severe growth failure associated with a novel heterozygous nonsense mutation in the GHR transmembrane domain leading to elevated growth hormone binding protein, Clin. Endocrinol. 92 (4) (2020) 331–337.
[24] D.M. Ornitz, P.J. Marie, Fibroblast growth factor signaling in skeletal development and disease, Genes Dev. 29 (14) (2015) 1463–1486.
[25] J. Baron, L. Sävendahl, F. De Luca, A. Dauber, M. Phillip, J.M. Wit, et al., Short and tall stature: a new paradigm emerges, Nat. Rev. Endocrinol. 11 (12) (2015) 735–746.
[26] A. David, V. Hwa, L.A. Metherell, I. Netchine, C. Camacho-Hübner, A.J. Clark, et al., Evidence for a continuum of genetic, phenotypic, and biochemical abnormalities in children with growth hormone insensitivity, Endocr. Rev. 32 (4) (2011) 472–497.
[27] H.L. Storr, S. Chatterjee, L.A. Metherell, C. Foley, R.G. Rosenfeld, P.F. Backeljauw, et al., Nonclassical GH insensitivity: characterization of mild abnormalities of GH action, Endocr. Rev. 40 (2) (2019) 476–505.
[28] V. Hwa, M. Fujimoto, G. Zhu, W. Gao, C. Foley, M. Kumbaji, et al., Genetic causes of growth hormone insensitivity beyond GHR, Rev. Endocr. Metab. Disord. 22 (1) (2021) 43–58.
[29] M. Dixit, S.B. Poudel, S. Yakar, Effects of GH/IGF axis on bone and cartilage, Mol. Cell. Endocrinol. 519 (2021) 111052.
[30] W.H. Daughaday, P. Rotwein, Insulin-like growth factors I and II. Peptide, messenger ribonucleic acid and gene structures, serum, and tissue concentrations, Endocr. Rev. 10 (1) (1989) 68–91.
[31] M. Koike, Y. Yamanaka, M. Inoue, H. Tanaka, R. Nishimura, Y. Seino, Insulin-like growth factor-1 rescues the mutated FGF receptor 3 (G380R) expressing ATDC5 cells from apoptosis through phosphatidylinositol 3-kinase and MAPK, J. Bone Miner. Res. 18 (11) (2003) 2043–2051.
[32] M. Párrizas, A.R. Saltiel, D. LeRoith, Insulin-like growth factor 1 inhibits apoptosis using the phosphatidylinositol 3'-kinase and mitogen-activated protein kinase pathways, J. Biol. Chem. 272 (1) (1997) 154–161.
[33] S.A. Coolican, D.S. Samuel, D.Z. Ewton, F.J. McWade, J.R. Florini, The mitogenic and myogenic actions of insulin-like growth factors utilize distinct signaling pathways, J. Biol. Chem. 272 (10) (1997) 6653–6662.
[34] T.M. Miller, M.G. Tansey, E.M. Johnson Jr., D.J. Creedon, Inhibition of phosphatidylinositol 3-kinase activity blocks depolarization- and insulin-like growth factor I-mediated survival of cerebellar granule cells, J. Biol. Chem. 272 (15) (1997) 9847–9853.
[35] J.F. Kuemmerle, T.L. Bushman, IGF-I stimulates intestinal muscle cell growth by activating distinct PI 3-kinase and MAP kinase pathways, Am. J. Physiol. 275 (1) (1998) G151–G158.
[36] S.R. Lamande, E.S. Ng, T.L. Cameron, L.H.W. Kung, L. Sampurno, L. Rowley, et al., Modeling human skeletal development using human pluripotent stem cells, Proc. Natl. Acad. Sci. U.S.A. 120 (19) (2023) e2211510120.
[37] K.E. White, J.M. Cabral, S.I. Davis, T. Fishburn, W.E. Evans, S. Ichikawa, et al., Mutations that cause osteoglophonic dysplasia define novel roles for FGFR1 in bone elongation, Am. J. Hum. Genet. 76 (2) (2005) 361–367.
[38] H.Y. Kim, J.M. Ko, Clinical management and emerging therapies of FGFR3-related skeletal dysplasia in childhood, Ann Pediatr Endocrinol Metab 27 (2) (2022) 90–97.
[39] M.C. Murton, E.L.A. Drane, D.M. Goff-Leggett, R. Shediac, J. O'Hara, M. Irving, et al., Burden and treatment of achondroplasia: a systematic literature review, Adv. Ther. 40 (9) (2023) 3639–3680.
[40] D.M. Galetaki, N. Merchant, A. Dauber, Novel therapies for growth disorders, Eur. J. Pediatr. 183 (3) (2024) 1121–1128.

[41] I. Gudernova, I. Vesela, L. Balek, M. Buchtova, H. Dosedelova, M. Kunova, et al., Multikinase activity of fibroblast growth factor receptor (FGFR) inhibitors SU5402, PD173074, AZD1480, AZD4547 and BGJ398 compromises the use of small chemicals targeting FGFR catalytic activity for therapy of short-stature syndromes, Hum. Mol. Genet. 25 (1) (2016) 9–23.
[42] T. Ozaki, T. Kawamoto, Y. Iimori, N. Takeshita, Y. Yamagishi, H. Nakamura, et al., Evaluation of FGFR inhibitor ASP5878 as a drug candidate for achondroplasia, Sci. Rep. 10 (1) (2020) 20915.
[43] N. Su, M. Jin, L. Chen, Role of FGF/FGFR signaling in skeletal development and homeostasis: learning from mouse models, Bone Res 2 (2014) 14003.
[44] R. Savarirayan, J.M. De Bergua, P. Arundel, H. McDevitt, V. Cormier-Daire, V. Saraff, et al., Infigratinib in children with achondroplasia: the PROPEL and PROPEL 2 studies, Ther Adv Musculoskelet Dis 14 (2022), 1759720x221084848.
[45] Y. Funakoshi, N. Hata, D. Kuga, R. Hatae, Y. Sangatsuda, Y. Fujioka, et al., Pediatric glioma: an update of diagnosis, biology, and treatment, Cancers 13 (4) (2021).
[46] B. Lehtinen, A. Raita, J. Kesseli, M. Annala, K. Nordfors, O. Yli-Harja, et al., Clinical association analysis of ependymomas and pilocytic astrocytomas reveals elevated FGFR3 and FGFR1 expression in aggressive ependymomas, BMC Cancer 17 (1) (2017) 310.
[47] S. Holzhauser, M. Lukoseviciute, T. Andonova, R.G. Ursu, T. Dalianis, M. Wickström, et al., Targeting fibroblast growth factor receptor (FGFR) and phosphoinositide 3-kinase (PI3K) signaling pathways in medulloblastoma cell lines, Anticancer Res. 40 (1) (2020) 53–66.